

Photochromism of naphthoflavylum. On the role of 4-OH hemiketal in flavylum network

Raquel Gavara, Vesselin Petrov, Virginia López, Fernando Pina*

REQUIMTE, Departamento de Química, Faculdade de Ciências e Tecnologia, Universidade Nova de Lisboa, 2829-516 Caparica, Portugal

ARTICLE INFO

Article history:

Received 28 October 2010

Received in revised form 28 February 2011

Accepted 5 March 2011

Available online 22 March 2011

Keywords:

Photochromism

Hemiketals

Multistate systems

Naphthoflavylum

Chalcones

ABSTRACT

Flavylum compounds suffer in aqueous solution the nucleophilic addition of water at moderately acidic pH values (hydration reaction). The hydration is possible in two positions, namely at position 2, forming hemiketal **B2**, and at position 4, forming hemiketal **B4**. **B2** can subsequently evolve to give the *cis*- and *trans*-chalcone species. At the present work the network of chemical reactions involving the naphthoflavylum compound in aqueous solution was studied by means pH jumps, stopped flow, continuous irradiation and flash photolysis. The equilibrium and rate constants of the system were calculated through a mathematical model. The species **B4** has a kinetic effect similar to the one observed for the quinoidal base (for flavylum dyes bearing acidic groups), *i.e.* **B4** is a kinetic product retarding the rate of equilibration. Flash photolysis experiments in comparison with reverse pH jumps results show that the appearance of the flavylum ion is faster in the photochemical-induced process than in the thermal one, suggesting an additional photochemical pathway (besides photoisomerization) after the excitation of the *trans*-chalcone.

© 2011 Elsevier B.V. All rights reserved.

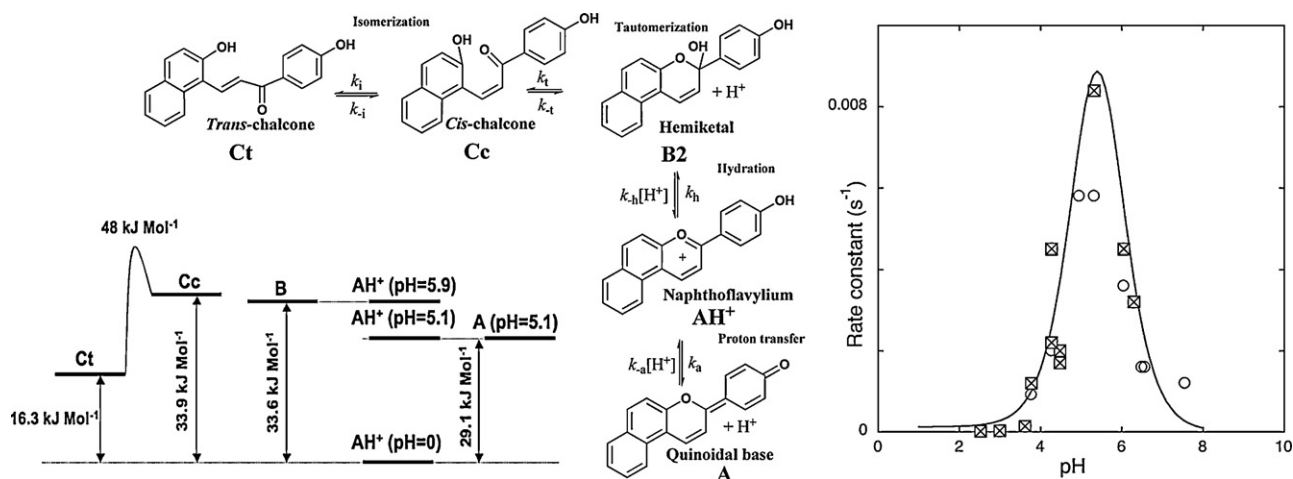
1. Introduction

The network of chemical reactions involving anthocyanins and related compounds has been shown to exhibit versatile applications [1–3]. Anthocyanins are the ubiquitous colorants used by Nature to obtain most of the red and blue colors in flowers and fruits [4]. Flavylum compounds are synthetic analogues of anthocyanins and present in aqueous solution the same general network of chemical reactions (Scheme 1) [5]. Flavylum ion (AH^+) is the most stable species in acidic solutions but when the pH is increased, the system evolves to a network of interconnected species. An important difference with anthocyanins, is that the *trans*-chalcone (**Ct**) is the most stable species at moderately acidic and neutral pH values. This form has the interesting property of photoisomerizing to the *cis*-chalcone (**Cc**) that at the appropriate pH value can then evolve to AH^+ or its quinoidal base (**A**), the most colorful species in the network. This photoreaction is reversible and the system reverts back to **Ct** in the dark. Therefore, both pH and light can be used for producing AH^+ and/or **A** from **Ct** in a reversible way. Due to these interesting properties flavylum compounds have been claimed as efficient photochromic systems [3] as well as models for optical memories and switches [6,7] the main factor ruling the final application being the magnitude of the *cis-trans* thermal barrier which depends strongly on the substituents.

The kinetics of the global process connecting AH^+ and **Ct** can be studied by means of pH jumps and flash photolysis experiments. When solutions of AH^+ ($\text{pH} < 1$) are submitted to a pH jump to higher values, (direct pH jumps) the quinoidal base is the first species to appear, because proton transfer to give **A** from AH^+ is by far the fastest process (at least five orders of magnitude) taking place in the network. One peculiarity of the system is the fact that at moderately acidic solutions **A** is a kinetic product that delays the formation of the final products (essentially **Ct**). In other words, **A** is not reactive (unless in basic solutions) towards **Ct** formation because the hemiketal **B2** results exclusively from the hydration of AH^+ . This means that at higher final pH values of the direct pH jump ($\text{pH} > \text{pK}_a$) more **A** and less AH^+ are formed and by consequence the rate to reach the final equilibrium becomes slower. On the other hand, direct pH jumps to lower pH's ($\text{pH} < \text{pK}_a$) results in more AH^+ (at the limit no reaction takes place), lower concentration of **Cc** to give **Ct** and the rate also decreases. The final result is a compromise between these two contradictory effects, a bell shape curve, Scheme 1 [8].

Regarding to the flash photolysis of **Ct**, three distinct kinetic processes are detected: (i) the faster is the formation of **Cc** from **Ct** that occurs during the flash, [9] (ii) the second is bi-exponential and corresponds to the formation of AH^+ /**A** (depending on pH). In some cases it is not possible to separate these two processes if one is much slower than the other because the former becomes the rate determining step, (iii) finally the photoproducts AH^+ /**A** revert back to **Ct** with a rate that follows the bell shape curve.

* Corresponding author. Tel.: +351 212948355; fax: +351 212948550.
E-mail address: fjp@dq.fct.unl.pt (F. Pina).



Scheme 1. (⊗) Recovery (slower) process of the flash photolysis; (○) direct pH jumps.

In the case of flavylum compounds, where no hydroxyl (or other acid) substituent is present, formation of another species, **B4**, (Scheme 2) resulting from hydration at position 4 of the flavylum cation, has been reported [10,11].

For flavylum compounds bearing the hydroxyl substituent, the hydration at position 4 is slower than proton transfer to give **A** and formation of **B4** usually is not significant if the quinoidal base is formed. The point is: while the hemiketal **B2** is effective in the formation of **Cc** and by consequence **Ct**, the species **B4** is also (like **A**) a kinetic product that retards the formation of the equilibrium products. On this basis a bell shape curve for the dependence of the rate constant to reach the equilibrium as a function of pH is also predicted. Many years ago McClelland in a seminal paper, reported the formation of **B4** in the case of flavylum itself, 4'-methoxyflavylum and 4'-methylflavylum [10]. However, these flavylum derivatives (in particular the 4'-methoxy) have a very high *cis-trans* isomerization barrier that allows **A**, **AH⁺**, **B2**, **B4** and **Cc** to reach a pseudo-equilibrium prior to the isomerization.

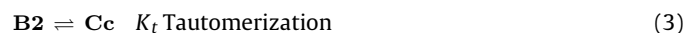
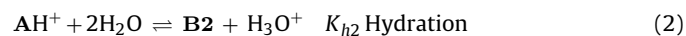
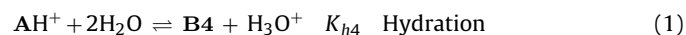
Recently it was reported that 4'-hydroxynaphthoflavylum follows the same sequence of chemical reactions firmly established for flavylum derivatives (Scheme 1), exhibiting also photochromism [5]. The objective of this work is to investigate the role played by the species **B4** in the case of the compound naphthoflavylum, [12,13] where a low thermal barrier is expected, Scheme 3.

2. Results and discussion

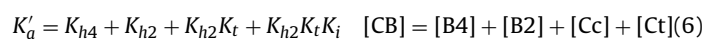
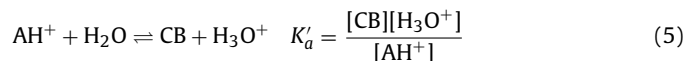
The spectral variations taken 30 s after a pH jump from stock solutions of **AH⁺** at pH < 1 to higher pH values is presented in Fig. 1A. Inspection of this figure shows the disappearance of the flavylum cation to give absorptions in the UV that are compatible with formation of **B4**, **B2** and **Cc** [14,15]. Equilibrated solutions after 4 h, Fig. 1B, show the characteristic pattern of an equilibrium between

AH⁺ ($\lambda_{\max} = 449$ nm) and essentially **Ct** ($\lambda_{\max} = 397$ nm). At higher pH values the equilibrium between **Ct** and its deprotonated form **Ct⁻** ($\lambda_{\max} = 485$ nm) takes place, Fig. 1C.

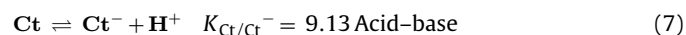
The sequence of reactions shown in Schemes 1 and 3 can be accounted for by the following set of elementary Eqs. (1)–(6)



Eqs. (1)–(4) can be substituted by a single acid–base equilibrium



In basic medium the following equilibrium also takes place



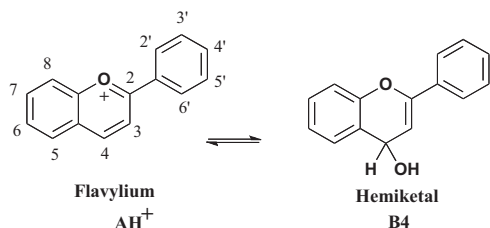
Considering that the hydrations and the tautomerization are faster enough to neglect the formation of **Ct** after 30 s the following relations, Eqs. (8) and (9), can be obtained from the fittings of Fig. 1A and B, respectively

$$\hat{K}'_a = K_{h2} + K_{h4} + K_{h2}K_t = 10^{-2.65} \quad (8)$$

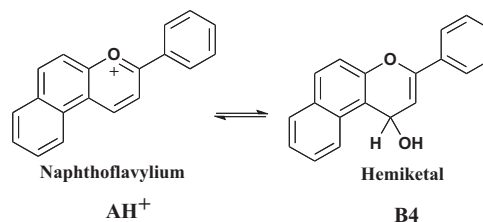
$$K'_a = K_{h2} + K_{h4} + K_{h2}K_t + K_{h2}K_tK_i = 10^{-1.6} \quad (9)$$

allowing to calculate

$$K_{h2}K_tK_i = 0.023 \quad (10)$$



Scheme 2.



Scheme 3.

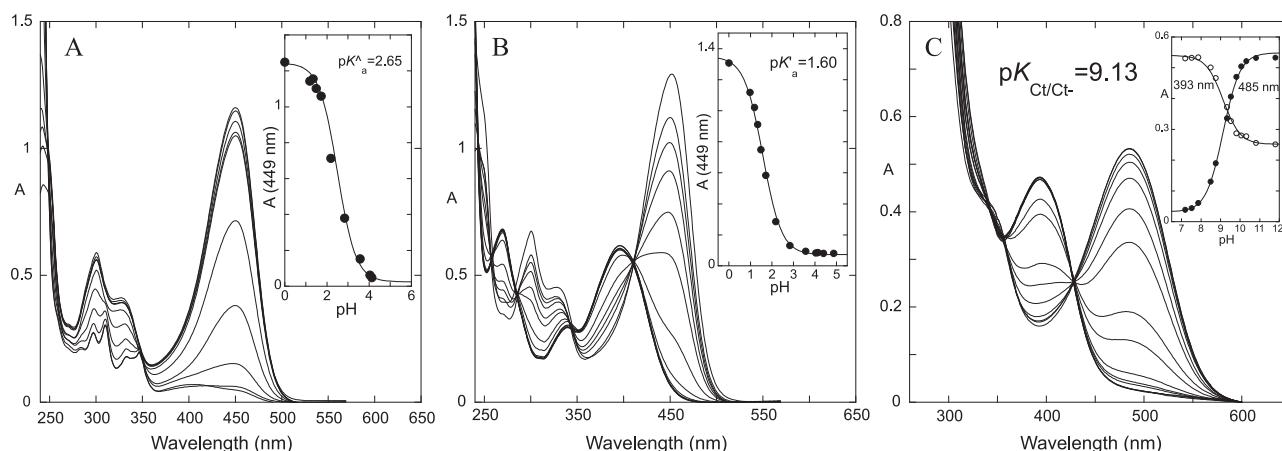


Fig. 1. (A) Spectral variations of the compound (4.4×10^{-5} M) taken circa 30 s after a pH jump from stock solutions of flavylum cation at pH = 0.6 in a mixture of ethanol:water (1:1); (B) equilibrated solutions (4 h), 5.0×10^{-5} M; (C) titration of the *trans*-chalcone (3.3×10^{-5} M).

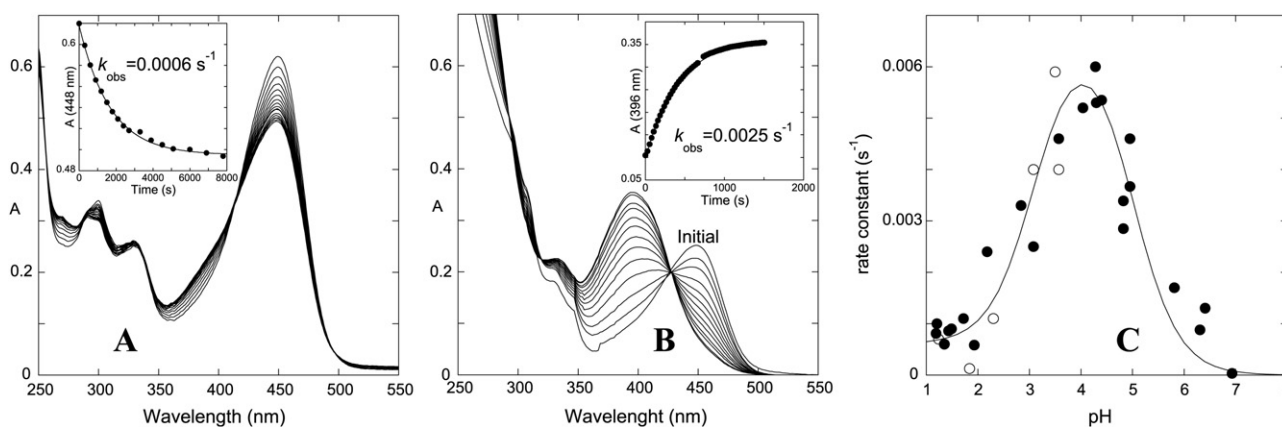


Fig. 2. Spectral variations upon direct pH jumps of naphthoflavylum, 3.3×10^{-5} M, from stock solutions at pH = 0.6 in a mixture of ethanol:water (1:1) to 1.35 (A) and 3.08 (B); rate constants of the direct pH jumps as function of pH (●) together with those of the thermal recovery after a flash photolysis (○), see below (C).

2.1. Direct pH jumps

Direct pH jumps have been carried out from stock solutions at pH = 0.6 in a mixture of ethanol:water (1:1) to higher pH values, Fig. 2 reporting those to 1.35 (A) and 3.08 (B).

As shown in Fig. 2 the final equilibrium corresponds to the disappearance of AH^+ to give Ct , their relative amounts occurring according to the observed $\text{pK}'_a = 1.60$. Representation of the rate constants of this process as a function of pH gives a bell shape curve similar to those previously reported for flavylum compounds with small *cis*–*trans* isomerization barriers and bearing a hydroxyl substituent. In other words, **B4** behaves similarly to **A**, being a kinetic product that retards the rate to reach the equilibrium at higher pH values, resulting in a bell shape curve as reported in Fig. 2C. The fitting of Fig. 2C was achieved by means of a mathematical procedure summarized in supplementary material [16]. In this fitting the constants obtained from the flash photolysis and reverse pH jumps experiments, see below, have been also taken into account. The equilibrium and rate constants are reported in Tables 1 and 2, respectively. In Table 2 the tautomerization values obtained through reverse pH jumps and flash photolysis, see below, are included.

Table 1
Equilibrium constants. Estimated error 20% unless other value is pointed out.

pK'_a	pK_a	K_{h2} (M^{-1})	K_{h4} (M^{-1})	K_t	K_i
1.60 ± 0.10	2.65 ± 0.10	6.5×10^{-4}	2.0×10^{-4}	1.9	22.2

2.2. Flash photolysis experiments: evidence for the formation of **B4**

Usually it is difficult to obtain spectral evidence for the formation of the transient species **B4**, because its absorption band occurs in the UV range and is overlapped by the absorption of the other species. However, **B4** can be detected by its influence on the kinetics of AH^+ formation in flash photolysis experiments. It has been widely reported that *trans*-chalcone photoisomerizes to give the *cis* analog [3,6,17] which can spontaneously form AH^+ at appropriate pH values. The traces of the absorption monitored immediately after the flash at 449 nm (AH^+ absorption) and 397 nm (Ct absorption) are represented respectively in Fig. 3A and B. The first process, taking place during the flash, is the bleaching due to the consumption of Ct to give Cc , which not show significant absorbance at these wavelengths (see Fig. 1A). At 449 nm the flavylum presents its absorption maximum but the *trans*-chalcone also absorbs ($\varepsilon_{\text{AH}^+}/\varepsilon_{\text{Ct}} = 16.4$), its contribution becoming significant because at this pH value Ct is higher than 90% of the overall species. The second process is attributed to the appearance of flavylum cation through the tautomerization of Cc to give B2 followed by the de-hydration of B2 and consequent AH^+ formation. This process occurs with a rate constant 1.15 s^{-1} and is detected not only at 449 but also at 397 nm, because the flavylum ion absorbs at the absorption maximum of Ct ($\varepsilon_{\text{Ct}}/\varepsilon_{\text{AH}^+} = 1.9$). The third and fourth kinetics correspond the disappearance of the AH^+ absorption. The third, 0.87 s^{-1} , can be explained only if AH^+ disappears to give **B4**, while the fourth is the usual back reaction of the photochromic

Table 2
Rate constants. Estimated error 20%.

k_{h2} (s ⁻¹)	k_{-h2} (M ⁻¹ s ⁻¹)	k_{h4} (s ⁻¹)	k_{-h4} (M ⁻¹ s ⁻¹)	k_t (s ⁻¹)	k_{-t} (s ⁻¹)	k_i (s ⁻¹)	k_{-i} (s ⁻¹)
0.85	1300	0.55	2800	0.19(0.89) ^a	0.1(0.47) ^a	0.01	4.5×10^{-4}

^a From flash.

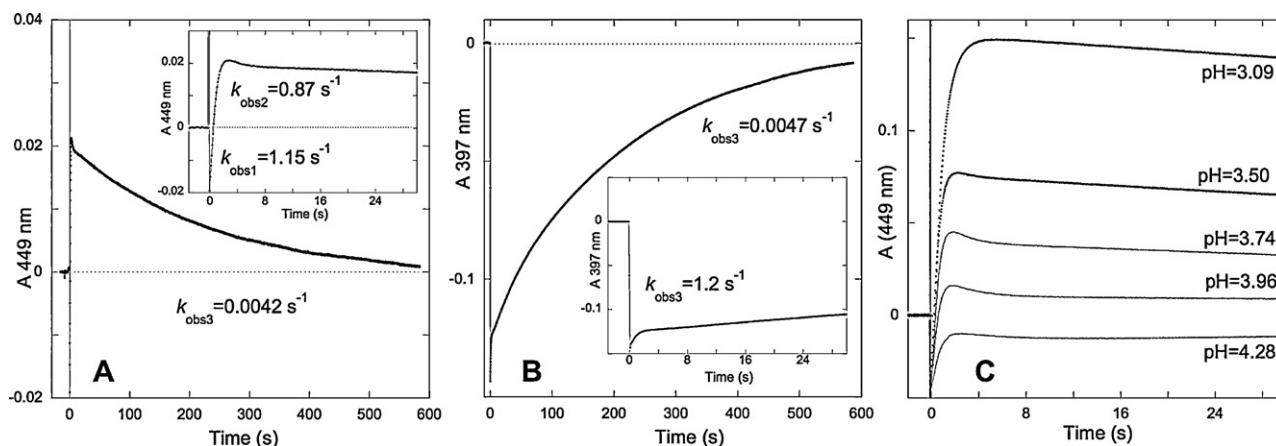


Fig. 3. Flash photolysis traces of a solution of the compound at pH = 3.57, followed at the flavylum absorption (A); *trans*-chalcone absorption (B); at different pH values at the flavylum absorption (C).

system returning to the equilibrium (that follows the bell shape curve in Fig. 2C). In other words, two types of pseudo equilibria are formed: (i) one involving **Cc**, **B2** and **AH⁺** (second kinetic process) and the other between **Cc**, **B2**, **AH⁺** and **B4** (corresponding to the third process). From this point the system reverts back to **Ct**. This interpretation is clearly corroborated by means of the experiments of Fig. 3C. The formation of **B4** is dependent on its pK_{h4} and is reliable to occur at higher pH values [10].

In Fig. 4 the rate constants of the kinetic process that can be monitored immediately after the flash are represented. As shown by McClelland and Gedge the tautomerization reaction is catalyzed by H⁺ as well as by OH⁻ [10]. This process can be the rate determining step of the global kinetics at low pH values, because the hydration due to its strong dependence on the proton concentration becomes very fast. In other words, after formation of **Cc** by the action of the flash, ring closure reaction of **Cc** to give **B2** (k_{-t}) becomes the controlling step of the bi-exponential process men-

tioned above (tautomerization/de-hydration), because at low pH values **B2** reacts much faster to give **AH⁺**. Fitting was achieved according to Eq. (11), allowing to conclude that $k_{-t} = 0.47 \text{ s}^{-1}$. The other values of Eq. (11) take into account the catalytic effect of acid and base. These values compare with $42 \text{ M}^{-1} \text{ s}^{-1}$ and $9.4 \times 10^{10} \text{ M}^{-1} \text{ s}^{-1}$ reported by McClelland for the flavylum ion.

$$k_{\text{obs}}(\text{Tautomerization} - \text{flash}) = 0.47 + 100[\text{H}^+] + 4 \times 10^{10}[\text{OH}^-] \quad (11)$$

The other limit situation occurs at higher pH values. At a certain point the hydration becomes the rate determining step of the process and the fitting is achieved with Eq. (12)

$$k_{\text{obs}}(\text{Hydration} - \text{flash}) = 0.85 + 1300[\text{H}^+] \quad (12)$$

2.3. Reverse pH Jumps

In the context of this work, reverse pH jumps are defined as the absorption traces obtained after a sequence of an initial pH jump from equilibrated solutions at pH = 0.6 in a mixture of ethanol:water to higher pH values, immediately followed by a pH jump back to acid (before formation of significant amounts of **Ct**). The objective of these studies is to get information about the pseudo-equilibrium that is formed (in a direct pH jump) before formation of **Ct**. Regarding the reverse pH jump from pH = 3.02 to pH = 1.42, Fig. 5A, it was observed an initial absorption (monitored at 450 nm) corresponding to 32% of the total flavylum as expected for a solution that was in a pseudo-equilibrium ($pK_a = 2.65$) between **AH⁺** by one side and **B2**, **B4** and **Cc**, by the other. The faster kinetic process is the formation of **AH⁺**, from **B2** and **B4**, and the second kinetic process is the formation of more **AH⁺** from **Cc** through **B2**. In Fig. 5B, the initial pH of the reverse pH jump was 6.45 and in this case no initial **AH⁺** was observed, as expected. The amplitudes of the traces are proportional to the amounts of **B2**+**B4** in comparison with **Cc**, Eq. (13).

$$\frac{[\text{Cc}]}{[\text{B2}] + [\text{B4}]} = 1.43 \quad (13)$$

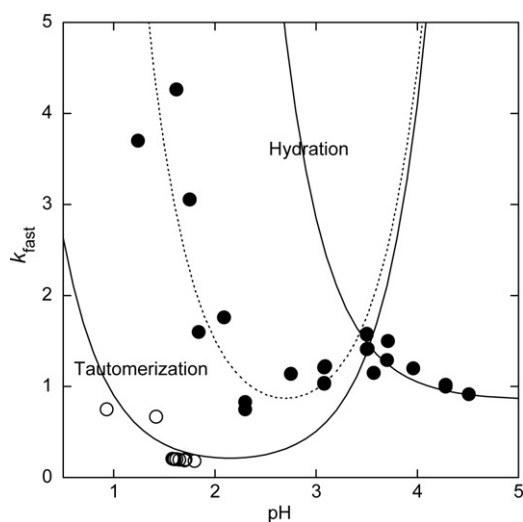


Fig. 4. Rate constants of the faster process observed after the flash as a function of pH (●). Rate constants of the reverse pH jumps (○).

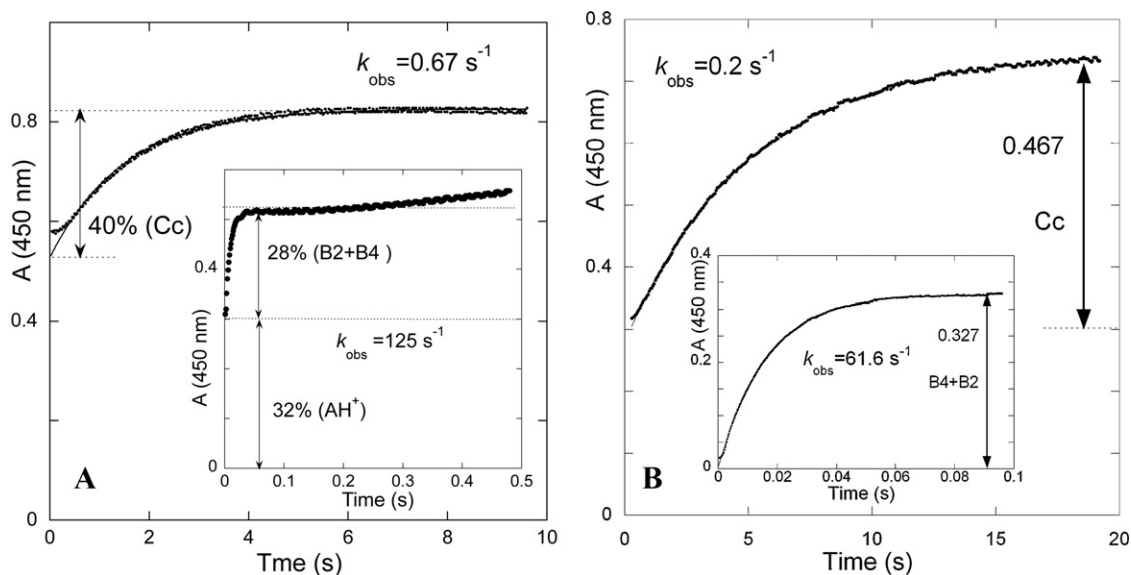


Fig. 5. Reverse pH jumps from solutions at pH = 3.02 to pH = 1.42 (A) and from pH = 6.45 to pH = 1.71 (B).

The rate constants of the faster process in the case of the reverse pH jumps should follow Eq. (14)

$$k_{\text{obs}} = k_{h2} + k_{h4} + k_{-h2}[\text{H}^+] + k_{-h4}[\text{H}^+] \quad (14)$$

The values for the hydration constant predicted by Eq. (14) on the basis of the data from Table 2, are 157 s^{-1} and 81 s^{-1} , respectively in reasonable agreement with the experimental values.

While the hydration process seems to be similar within experimental error in the pH jumps and flash photolysis experiments, the same does not occur for the tautomerization. The second and slower process of the reverse pH jumps is controlled by the tautomerization reaction: **B2** and **B4** at the pseudo-equilibrium are consumed during the first kinetics and the extra flavylum formed in the slower process takes place from **Cc** through **B2**, and should be also controlled by k_{-t} . However the fitting is achieved by Eq. (15).

$$k_{\text{obs}} = 0.1 + 8[\text{H}^+] + 4 \times 10^{10}[\text{H}^+] \quad (15)$$

Fig. 5 shows that the tautomerization process (the rate determining step at higher proton concentrations) is not the same when flavylum is obtained after a light flash or through a reverse pH jump. It is worth mentioning that the value obtained for k_{-t} by means of the latter is in good agreement with the value reported previously for 4-hydroxynaphthoflavylum [5].

According to the experimental data the photochemical process is faster than the thermal one. This can be explained only if the photochemical process takes place through a different pathway. The question is which intermediate(s) are involved in this process. Scheme 4 shows some additional processes that could occur together with photoisomerization in acidic medium. One possibility could be the formation of the *trans*-enol that would isomerize easily to the *cis*-enol and lead to **B2**. However, this pathway would imply a slow keto-enol tautomerization in the *cis* species, which in principle is not expected. One possible alternative is the formation of a diene intermediate **I** through a sigmatropic hydrogen shift induced by light. A similar structure was proposed by several authors in the framework of chromene photochemistry [18–21]. This intermediate could subsequently cyclize as shown in Scheme 4. Moreover, it is worth pointing out that this additional pathway is only participating in *one way*, *i.e.* to form **AH⁺**, and it is not active during the thermal recovery to **Ct** because, as mentioned above, the thermal recovery is in agreement with the rate measured in the direct pH jumps.

2.4. Continuous irradiations

The photochromic behavior of the system was studied by means of continuous irradiation. Equilibrated solutions of the *trans*-chalcone at moderately acidic pH values were irradiated at 397 nm leading to the (reversible) formation of flavylum cation. The quantum yields of the photochemical process are represented in Fig. 6 and are in agreement with Eq. (16), which assumes that the pseudo-equilibrium involving **AH⁺**, **B2**, **Cc** and **B4** is achieved after the excitation of **Ct**.

$$\Phi = \Phi_0 \frac{[\text{H}^+]}{[\text{H}^+] + K_a'} \quad (16)$$

Fitting of Eq. (16) was achieved for $\Phi_0 = 0.125$ and $\text{p}K_a' = 2.65$ in perfect agreement with the pseudo-equilibrium constant. Eq. (16) reflects the fraction of flavylum cation that is formed upon photo-induced reaction of **Ct**. In other words, after the irradiation **Cc** equilibrates with **B2**, **B4** and **AH⁺** before reverting back to **Ct** through the thermal recovery process of the photochromic system, see Scheme 5.

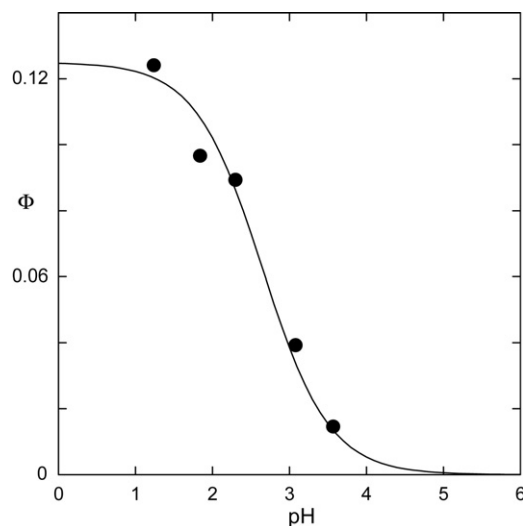
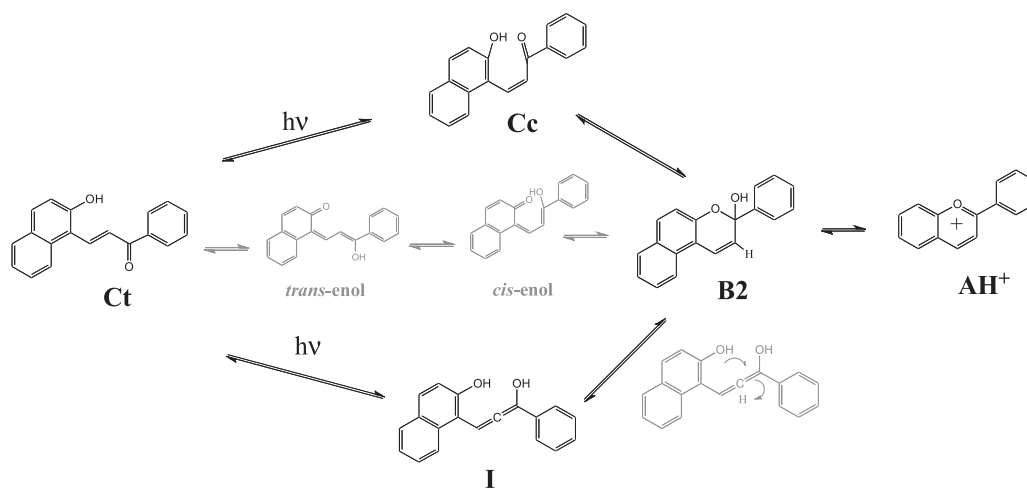
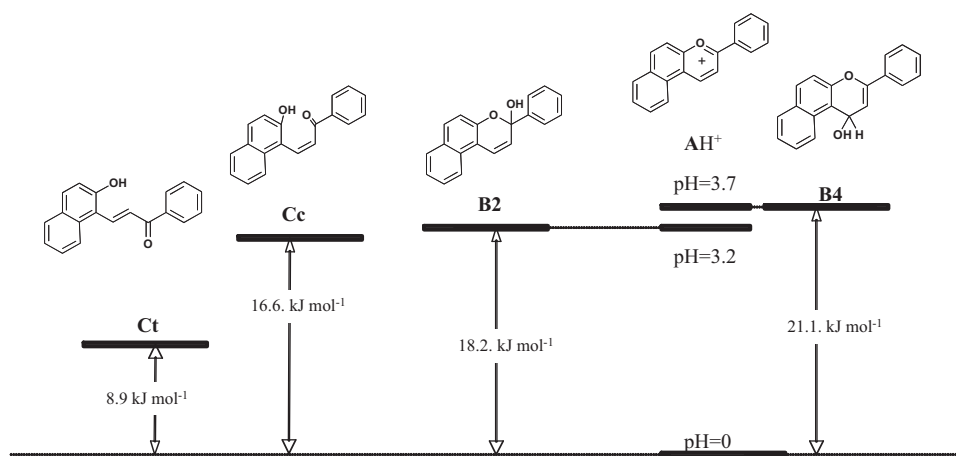


Fig. 6. Quantum yields for flavylum formation $\lambda_{\text{irr}} = 397 \text{ nm}$. $I_0 = 2.9 \times 10^{-7} \text{ Einstein min}^{-1}$.



Scheme 4.



Scheme 5.

2.5. Fluorescence emission

The fluorescence emission spectrum of the flavylum cation is shown in Fig. 7A. Representation of the emission as a function of pH leads to a curve that inflects at higher pH values as the pK'_a ,

as expected for a system without excited state proton transfer. The fluorescence emission curves are coincident with those obtained by UV–vis absorption. At lower pH values the quenching of the fluorescence takes place due to proton quenching, a phenomenon reported by Weller [22] and Harris and Selinger [23] many years ago, Fig. 7B.

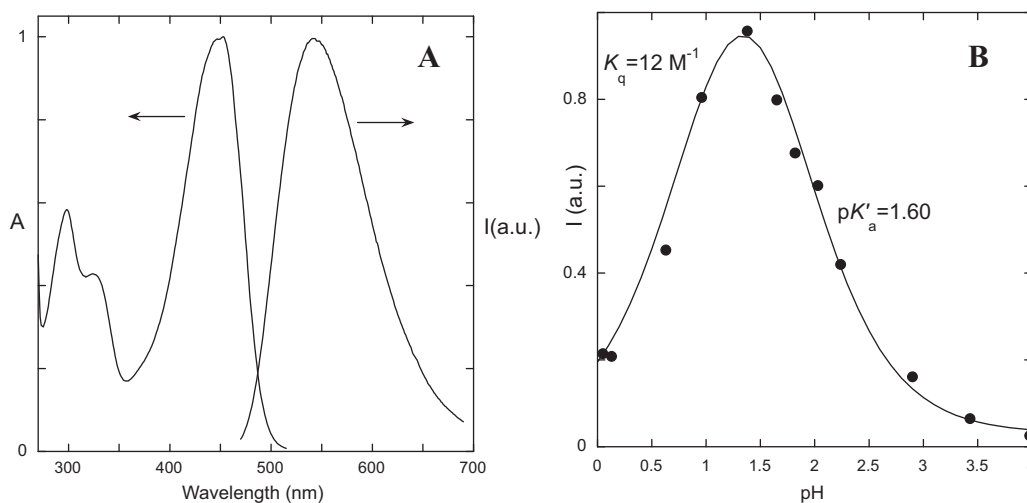


Fig. 7. Normalized excitation and emission spectra for AH⁺ (A) and fluorescence quenching depending on pH (B).

The fitting of the data in Fig. 7B was obtained by the following expression:

$$I = \frac{2.2}{1 + 12[\text{H}^+]} \times \frac{[\text{H}^+]}{[\text{H}^+] + 10^{-1.65}} \quad (17)$$

where I is the observed fluorescence intensity and 2.2 the fluorescence intensity in the absence of the quencher (H^+).

In Eq. (17) the first term is equivalent to the Stern–Volmer expression and the second is the mole fraction distribution of the flavylum cation. On this basis the Stern–Volmer constant is equal to 12 M^{-1} .

3. Conclusion

The rate of the conversion between flavylum cation and *trans*-chalcone shows a bell shape curve as a function of pH. The effect of **B4** formation is similar to the quinoidal base, being a kinetic product that retards the conversion of **AH**⁺ into **Ct**. An interesting feature of this network of chemical reactions is the fact that the kinetics of flavylum cation formation from **Cc** and **B2** by a thermal process (reverse pH jumps) is slower than upon absorption of a light flash (flash photolysis). Finally, the thermodynamic energy level diagram of the network of the present compound, Scheme 5, compared with the one of 4'-hydroxynaphthoflavylum, [5] Scheme 1, reflects the relative stabilization of flavylum cation in the last due to the electron donor character of the hydroxyl substituent. The fact that naphthoflavylum compounds follow the same network of chemical reactions of flavylum compounds, in particular exhibiting photo induced *trans*–*cis* isomerization, extends the number of compounds possessing photochromism and the possibility of shifting the color of the photoproduct to higher wavelengths.

4. Experimental

4.1. Synthesis

All reagents and solvents used were of analytical grade. The NMR spectra at 298.0 K were obtained on a Bruker AMX400 operating at 400.13 (¹H) and 100 MHz (¹³C) and deuterated solvents were used as an internal reference. Matrix-Assisted Laser Desorption/Ionization-Time-Of-Flight-Mass (MALDI-TOF-MS) analyses were performed with the positive reflector mode. The apparatus used is a Voyager-DETM PROBiospectrometry Workstation model (Applied Biosystems) and data were analysed with Voyager V5.1 software. Naphthoflavylum tetrafluoroborate was prepared from 2-hydroxy-1-naphthaldehyde and acetophenone using the method developed by Katritzky et al. [24] which employs an acidic mixture composed by acetic acid, acetic anhydride and HBF_4 instead of the traditional gaseous HCl [12]. ¹H RMN (400.13 MHz, 298.0 K, $\text{CD}_3\text{OD}/\text{D}_2\text{O}(1:1)$, $\text{pD} < 1$) δ (ppm): 10.05 (1H, d, ³J = 9.2 Hz), 8.77–8.74 (2H, m), 8.72 (1H, d, ³J = 9.6 Hz), 8.44 (2H, d, ³J = 7.6 Hz), 8.17 (1H, d, ³J = 9.2 Hz), 8.13 (1H, d, ³J = 8.0 Hz), 7.95 (1H, t, ³J = 7.4 Hz), 7.86–7.78 (2H, m), 7.74 (2H, t, ³J = 8.0, ⁴J = 7.6 Hz); ¹³C RMN (100 MHz, 298.0 K, $\text{CD}_3\text{OD}/\text{D}_2\text{O}(1:1)$, $\text{pD} < 1$) δ (ppm): 173.05, 159.57, 151.92, 144.75, 137.98, 132.37, 132.22, 131.29, 131.09, 130.43, 129.06, 128.26, 124.47, 123.93, 117.90, 117.67; MS (MALDI-TOF): m/z (%): calcd for $\text{C}_{19}\text{H}_{13}\text{O}^+$: 257.10; found: 257.15 (100).

4.2. Measurements

Solutions were prepared using Millipore water and spectroscopic ethanol. The solution pH was adjusted by addition of HCl,

NaOH and the universal buffer of Theorell and Stenhagen [25] and was measured on a Metrohm 713 pH meter which has a combined glass electrode. UV–vis absorption spectra were recorded on a Varian–Cary 100 Bio spectrophotometer, a Varian–Cary 5000i or a Shimadzu VC2501-PC. Flash photolysis experiments were carried out as reported previously [8]. Reverse pH jumps experiments were carried out on a SX20 stopped-flow spectrometer (Applied Photophysics). Photoexcitation in continuous irradiation experiments were carried out using a Xe lamp (150 W , $\lambda_{\text{irr}} = 397 \text{ nm}$) and the incident light intensity was measured by ferrioxalate actinometry [26]. Fluorescence spectra were acquired on a Jobin Yvon Spex, Fluorolog FL3-22.

Acknowledgements

FCT-MCTES is also acknowledged for financial support through projects PTDC/QUI/67786/2006 and PTDC/QUI-QUI/104129/2008 and Post-doc grants SFRH/BPD/44639/2008 (RG) and SFRH/BPD/18214/2004 (VP).

Appendix A. Supplementary data

Supplementary data associated with this article can be found, in the online version, at doi:10.1016/j.jphotochem.2011.03.002.

References

- [1] T. Swain, in: J.B. Harborne, T.J. Mabry, H. Mabry (Eds.), *The Flavonoids*, Chapman and Hall/CRC Press, London, 1975, pp. 1096–1129.
- [2] R. Brouillard, O. Dangles, in: J.B. Harborne (Ed.), *The Flavonoids: Advances in Research Since*, Chapman and Hall/CRC Press, New York, 1986, pp. 565–588.
- [3] F. Pina, M. Maestri, V. Balzani, in: H.S. Nalwa (Ed.), *Handbook of Photochemistry and Photobiology*, 3, American Scientific Publishers, Stevenson Ranch, CA, 2003, pp. 411–449, Chapter 9.
- [4] P. Markakis (Ed.), *Anthocyanins as Food Colors*, Academic Press, New York, 1982.
- [5] R. Gavara, V. Petrov, F. Pina, *Photochem. Photobiol. Sci.* 9 (2010) 298–303.
- [6] M. Maestri, F. Pina, V. Balzani, in: B.L. Feringa (Ed.), *Molecular Switches*, Weinheim, Wiley-VCH, 2001, pp. 309–334.
- [7] E. Bogdan, L. Rougier, L. Ducasse, B. Champagne, F. Castet, *J. Phys. Chem. A* 114 (2010) 8474–8479.
- [8] F. Pina, M.J. Melo, R. Ballardini, L. Flamigni, M. Maestri, *New J. Chem.* 21 (1997) 969–976.
- [9] Not detected in our nano-second flash photolysis apparatus.
- [10] R.A. McClelland, S. Gedge, *J. Am. Chem. Soc.* 102 (1980) 5838–5848.
- [11] V. Petrov, R. Gomes, A.J. Parola, F. Pina, *Dyes Pigments* 80 (2009) 149–155.
- [12] A. Russell, J.C. Speck, *J. Am. Chem. Soc.* 63 (1941) 851–852.
- [13] M. Elhabiri, P. Figueiredo, F. George, J.-P. Cornard, A. Fougereuse, J.-C. Merlin, R. Brouillard, *Can. J. Chem.* 74 (1996) 697–706.
- [14] M. Maestri, F. Pina, A. Roque, P. Passaniti, *J. Photochem. Photobiol. A: Chem.* 137 (2000) 21–28.
- [15] F. Pina, M.J. Melo, M. Maestri, P. Passaniti, N. Camaioni, V. Balzani, *Eur. J. Org. Chem.* (1999) 3199–3207.
- [16] V. Petrov, F. Pina, *J. Math. Chem.* 47 (2010) 1005–1026.
- [17] A recent example: Y. Leydet, A.J. Parola, F. Pina, *Chem. -Eur. J.* 16 (2010) 545–555.
- [18] S. Delbaere, J.-C. Micheau, G. Vermeersch, *Org. Lett.* 4 (2002) 3143–3145.
- [19] S. Delbaere, J.-C. Micheau, G. Vermeersch, *J. Org. Chem.* 68 (2003) 8968–8973.
- [20] G. Favaro, A. Romani, F. Ortica, *Photochem. Photobiol. Sci.* 2 (2003) 1032–1037.
- [21] F. Ortica, P. Smimmo, G. Favaro, U. Mazzucato, S. Delbaere, D. Venec, G. Vermeersch, M. Frigoli, C. Moustrou, A. Samat, *Photochem. Photobiol. Sci.* 3 (2004) 878–885.
- [22] A. Weller, *Z. Phys. Chem.* 17 (1958) 224–245.
- [23] C.M. Harris, B.K. Selinger, *J. Phys. Chem.* 84 (1980) 891–898.
- [24] A.R. Katritzky, P. Czerney, J.R. Lndevell, W.H. Du, *Eur. J. Org. Chem.* (1998) 2623–2629.
- [25] F.W. Küster, A. Thiel, A. Ruland, *Tabelle per le Analisi Chimiche e Chimico-Fisiche*, 12th ed., Hoepli, Milano, 1982, pp. 157–160.
- [26] C.G. Hatchard, C.A. Parker, *Proc. R. Soc. Lond. Ser. A* 235 (1956) 518.